FIRE: Fast Iris REcognition on mobile phones by combining colour and texture features.

Chiara Galdi[a,**], Jean-Luc Dugelay[a]

[a] *EURECOM, Campus SophiaTech, 450 Route des Chappes, CS 50193 06904 Biot Sophia Antipolis cedex, FRANCE*

ABSTRACT

FIRE is a Fast Iris REcognition algorithm especially designed for iris recognition on mobile phones under visible-light. It is based on the combination of three classifiers exploiting the iris colour and texture information. Its limited computational time makes FIRE particularly suitable for fast user verification on mobile devices. The high parallelism of the code allows its use also on large databases. FIRE, in its first version, was submitted to the Mobile Iris CHallenge Evaluation part II held in 2016. In this paper, FIRE is further improved: a number of different techniques has been analyzed and the best performing ones have been selected for fusion at score level. Performance are assessed in terms of Recognition Rate (RR), Area Under Receiver Operating Characteristic Curve (AUC), and Equal Error Rate (EER).

1. Introduction

The need of secure use of data and services joined to the ever-increasing technological development of the imaging sensors led to the spread of biometric recognition systems on new devices. Mobile phones have the main advantage of being portable, ever more computationally powerful, and equipped with high resolution cameras. Providing a secure and accurate way to get authenticated at any moment and from any place is of utmost interest nowadays. However, there are a number of issues related to iris recognition on mobile devices, originating from the fact that the acquisition of the iris image is performed in unconstrained settings, such as out-of-focus images, specular or diffuse reflections, eyelid or eyelash occlusions, low resolution images, etc. (Proenca and Alexandre (2007); DeMarsico et al. (2012)). This kind of images are called "noisy", and require ad hoc solutions e.g. segmentation algorithm and feature extractor, particularly designed for "noisy iris recognition".

A novel technique for noisy iris segmentation exploiting the Watershed transform has been presented in Abate et al. (2015), while a solution for secure home banking based on user iris verification using a mobile device, i.e. a tablet, is presented in DeMarsico et al. (2014). In Barra et al. (2015), a novel

approach based on the use of spatial histograms is presented. Other biometric traits has been also exploited for user recognition on mobile devices, including ear recognition in Fahmi et al. (2012), gait in Nickel et al. (2012), keystroke and finger pressure in Saevanee and Bhattarakosol (2009), arm movement when answering or placing a call in Conti et al. (2011), speech, alone or in combination with other biometrics, in Mohanta and Mohapatra (2014) and Poh et al. (2013), and 3d face recognition in Raghavendra et al. (2013).

An important aspect of the proposed approach, is its suitability for iris recognition under visible light, taking into consideration the fact that there are many application scenarios in which Near Infra Red (NIR) illumination is not available or applicable. For example for continuous re-identification, i.e. when the system continuously verifies the user identity, in which case the user cannot be constantly exposed to NIR light, since the effects of a prolonged exposure to NIR light are still uncertain. Another example scenario in which NIR illumination cannot be available is for forensic, i.e. the process of analyzing images or videos from different sources to off-line verification of the identity of a person.

In this paper, we present FIRE, a novel approach for iris recognition particularly designed for iris recognition on smartphones and presented to the MICHE II - Mobile Iris CHallenge Evaluation Part II, held in 2016 [1]. The algorithm is based on

---

**Corresponding author: Tel.: +33 (0)4 93 00 81 67; fax: +33 (0)4 93 00 82 00;
e-mail: chiara.galdi@eurecom.fr (Chiara Galdi)

[1]http://biplab.unisa.it/MICHE_Contest_ICPR2016/index.php

the combination of three feature extractors, each of which describes a different characteristic of the iris: an iris colour descriptor, an iris texture descriptor, and an iris colour spot (hereinafter "cluster") descriptor. FIRE is tested on the MICHE-I[2], an iris image database collected with different mobile devices DeMarsico et al. (2015).

The key features of the proposed method are: (i) the use of the colour information (only available when using visible light illumination), (ii) the suitability for noisy iris recognition, (iii) the limited computational time, and (iv) the high parallelization of the code.

In this paper we present the new experiments carried out, consisting in testing different techniques for the colour and texture feature extraction, and the corresponding evaluation in terms of Recognition Rate (RR), Area Under Receiver Operating Characteristic Curve (AUC), and Equal Error Rate (EER).

The remainder of the paper is organized as follows: in section 2, the multi-classifier algorithm is described; in section 3 the experimental setting is described in order to assure experiment reproducibility. In section 4 the experimental results are presented and section 5 concludes the paper.

2. Colour and texture feature based multi-classifier

The iris presents a complex pattern made up of many distinctive features such as arching ligaments, furrows, ridges, crypts, rings, corona, freckles, and a zigzag collarette Daugman (2004), some of which may be seen in Fig. 2 (left). However, in order to capture these minute characteristics, it is necessary to have a high quality imaging sensor, adequate lighting conditions, a small distance between the eye and the sensor.

For the design of the proposed approach, we focused on those characteristics that are more likely to be observable on iris images captured under visible light and by mobile devices, see Fig. 2 (right). We analyzed the images collected in the MICHE-I database and observed that: colour is for sure a discriminative feature, even if not sufficient to uniquely distinguish an individual; in these kind of images, the texture is less clear compared to NIR iris images; some macro-features easily detectable on noisy images, such as colour spots (see Fig. 4 as reference) can help in the recognition process.

The proposed solution is a multi-classifier approach, combining features of different nature in order to maximize the performances by exploiting as much as possible the information that is possible to retrieve from noisy iris images. FIRE is made up of three descriptors, namely the colour descriptor, the texture descriptor and the cluster descriptor. In figure 1, a flow chart describing the proposed approach is given.

2.1. Colour descriptor

Iris image databases can be distinguished in two main categories, those acquired under Near Infra Red (NIR) illumination and those captured under Visible Light (VL). NIR databases are composed by gray scale images, see Fig. 2 as reference.
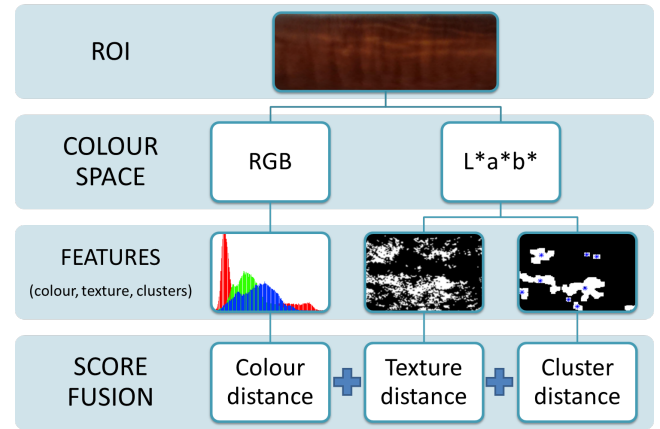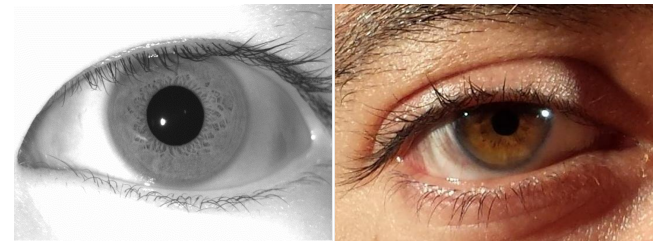

Fig. 1. Algorithm flow chart.

Fig. 2. Examples of iris acquisition, under near infra red illumination (left, from the Gender From Iris (GFI) Dataset, Tapia et al. (2016)) and under visible light (right).

The MICHE-I database, on which the MICHE II participants were asked to test their approaches, has been acquired under VL. Thus, the colour information can be exploited to improve the recognition performances. A number of colour metrics have been tested and are described in the following. A MATLAB implementation by Boris Schauerte[3] of the colour distances presented in Rubner et al. (2000), has been employed.

Given two irises, each picture is first split in small blocks and for each pair of corresponding blocks, the colour distance is computed. The minimum colour distance obtained is the final score returned by the colour descriptor.

2.1.1. Colour histogram distance

The first colour descriptor is based on a technique designed for image retrieval in image databases. The Euclidean distance between the colour histograms of the two images to be compared is computed as follows:

$$d(h, g) = \sqrt{\sum_A \sum_B \sum_C (h(a, b, c) - g(a, b, c))^2}$$

where h and g represent the two colour histograms and (a, b, c) represent the three colour channels, rgb in our case.

2.1.2. Chi square statistics

This distance measures how unlikely it is that one distribution was drawn from the population represented by the other.
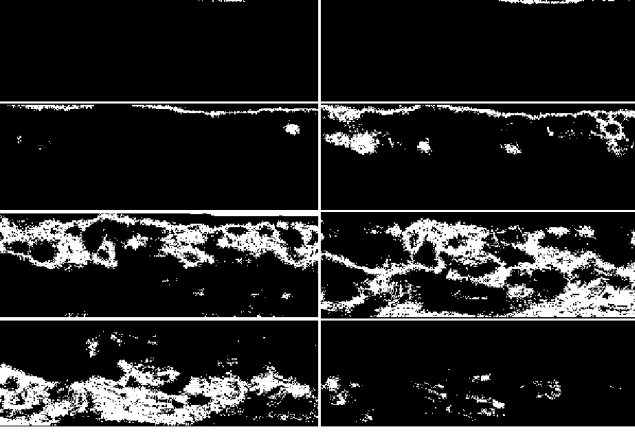
Fig. 3. Iris image multi-layer decomposition: the 8 layers obtained from the colour channel a^*.

Fig. 4. Iris colour spots examples.

The chi square statistics is defined as follows:

$$d_{\chi^2}(H, K) = \sum_i \frac{(h_i - m_i)^2}{m_i}$$

where $m_i = \frac{h_i + k_i}{2}$.

2.1.3. Histogram intersection

The histogram intersection (Swain and Ballard (1991)) can handle partial matches when the areas of the two histograms are different.

$$d_\cap(H, K) = 1 - \frac{\sum_i min(h_i, k_i)}{\sum_i k_i}$$

2.1.4. Match distance

The match distance, Shen and Wong (1983), between two one-dimensional histograms is defined as the Minkowski distance of order 1 between their corresponding cumulative histograms. The match distance cannot handle partial matches and does not extend to higher dimensions because the relation $j \leq i$ is not a total ordering in more than one dimension, and the resulting arbitrariness causes problems.

$$d_M(H, K) = \sum_i |\hat{h}_i - \hat{k}_i|$$

where $\hat{h}_i = \sum_{j \leq i} h_j$ is the cumulative histogram of $\{h_i\}$, and similarly for $\{k_i\}$.

2.1.5. Kolmogorov-Smirnov distance

The Kolmogorov-Smirnov distance is a common statistical measure for unbinned distributions. Similarly to the match distance, it is defined only for one dimension.

$$d_{KS}(H, K) = \max_i(|\hat{h}_i - \hat{k}_i|)$$

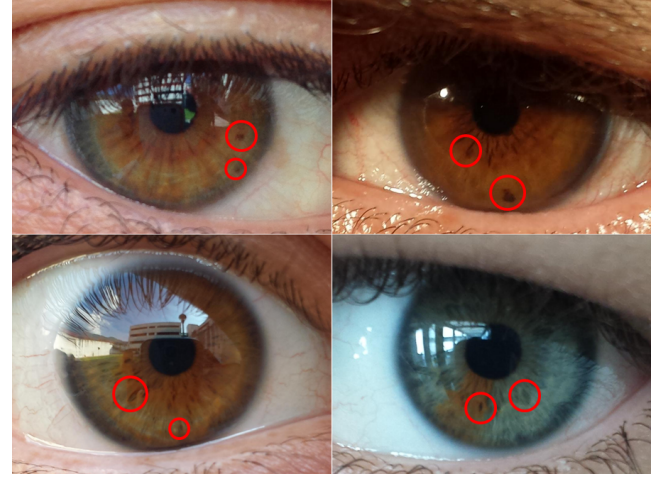Where $\hat{h}_i$ and $\hat{k}_i$ are cumulative histograms.

2.2. Texture descriptor

The texture descriptor is based on the computation of the Minkowski-Bouligand dimension, also known as box-counting dimension. The box-counting dimension of a set S is defined as follows:

$$dim_{box}(S) := lim_{\varepsilon \to 0} \frac{logN(\varepsilon)}{log(\frac{1}{\varepsilon})}$$

where $N(\varepsilon)$ is the number of boxes of side length ε required to cover the set S.

The input image is first divided into several layers obtained by a decomposition process illustrated in the following. Each layer l_i, where $i = 1, 2, ..., N$ and N is the number of layers, is further divided in small blocks $b_{i,j}$, where i is the corresponding layer and $j = 1, 2, ..., M$ and M is the number of blocks. For each block $b_{i,j}$, the corresponding box-counting dimension $d_{b_{i,j}}$ is computed. Finally, the distances $d_{b_{i,j}}$ are concatenated in a feature vector.

Feature vectors coming from different iris images are compared through the Euclidean distance.

2.2.1. Multi-layer iris image decomposition

The input iris image is first projected in the CIE 1976 $L^*a^*b^*$ colour space, where L^* is the lightness dimension and a^* and b^* are the colour-opponent dimensions.

Only the colour dimensions are further processed since the lightness information is more likely to be different also among images of the same iris, e.g. if the lighting conditions have changed between the acquisitions of the same user.

For each colour channel (a^* and b^*) the values are first normalized between 0 and 255, then the resulting grey values are divided in 8 intervals of size 32 (32*8 = 256), i.e. 8 layers are obtained from each colour channel, where the first layer contains the pixels with values in [0, 31], the second in [32, 63], ..., and the last in [224, 255]. For each layer, the value of the pixels belonging to the corresponding interval are set to 1 while all the others are set to 0. A sample iris image multi-layer decomposition is given in figure 3.
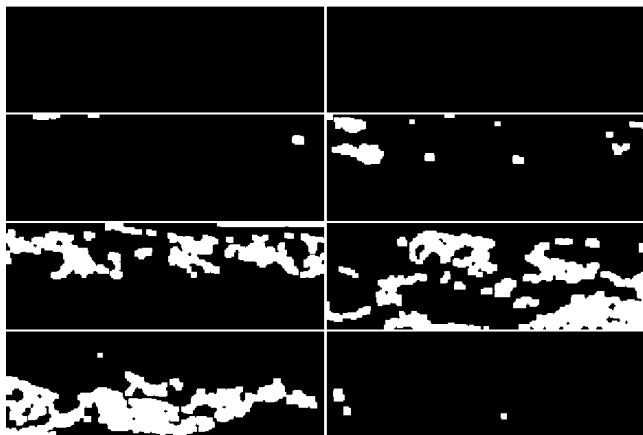
Fig. 5. Iris clusters representation on the layers originating from the image decomposition: clusters on the a^* colour channel.

2.3. Cluster descriptor

We use the term "clusters" to indicate the small colour spots that characterize some human irises. When two irises are similar in terms of colour (or seem similar because the image is in grey scale) humans leverage on these small spots to determine whether the observed images belong to the same iris or not. In figure 4, it is possible to observe some of these colour spots. The two irises in the first column, for example, are very similar in terms of colour, but the darker colour spots (circled in red in the image) allow the observer to distinguish them.

In order to extract and represent these clusters, the input iris image is first processed by the multi-layer decomposition previously illustrated in section 2.2.1. For each layer, a closing morphological operation, followed by an opening, is performed. The resulting clusters are the connected components (white pixels) showed in the example in figure 5.

For each cluster, the following properties are computed (by using the MATLAB function *regionprops*):

- Centroid coordinates;

- Orientation;

- Eccentricity.

In figure 6, the centroids and corresponding ellipsis are plotted for each cluster of a given layer.

For each cluster, a cluster feature vector (hereinafter CFV) is obtained by concatenating the cluster property listed above. For each layer, a list of CFVs is obtained. When two iris images have to be compared, for each pair of corresponding layers, the two lists of CFVs are matched following an all-versus-all scheme and the average distance of the best matching pairs (i.e. the pair of clusters with minimum distance) is computed. Thus, a distance value for each pair of corresponding layers is obtained, the final score is given by averaging them.

3. Experimental setting

In this section some implementation details are given and the results of the new set of experiments are compared with the ones obtained in the MICHE II contest.
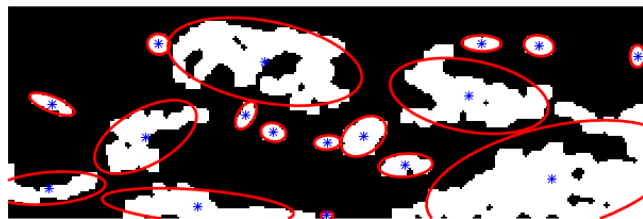

Fig. 6. Cluster centroids visualization.

Fig. 7. Colour normalization: in the first row some original pictures from the MICHE-I database are shown; the second row illustrates the same pictures after colour normalization.
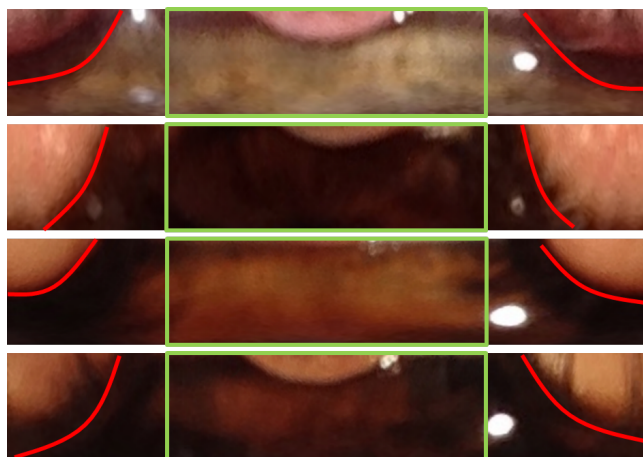

Fig. 8. ROI selection on 4 sample images of the MICHE-I DB: in green, the ROI selected from the iris image; in red, the eyelid occlusions.

3.1. Dataset description and preprocessing

The database employed for the MICHE II challenge is the MICHE-I database, a large set of iris images captured by different mobile devices in different and unconstrained conditions, see DeMarsico et al. (2015) for reference. A subsection of the MICHE-I database composed by 120 iris images from 30 different individuals, was made available to the MICHE II participants on the contest web site. More details on the performance evaluation can be found on the competition web site [4]. The im-

---

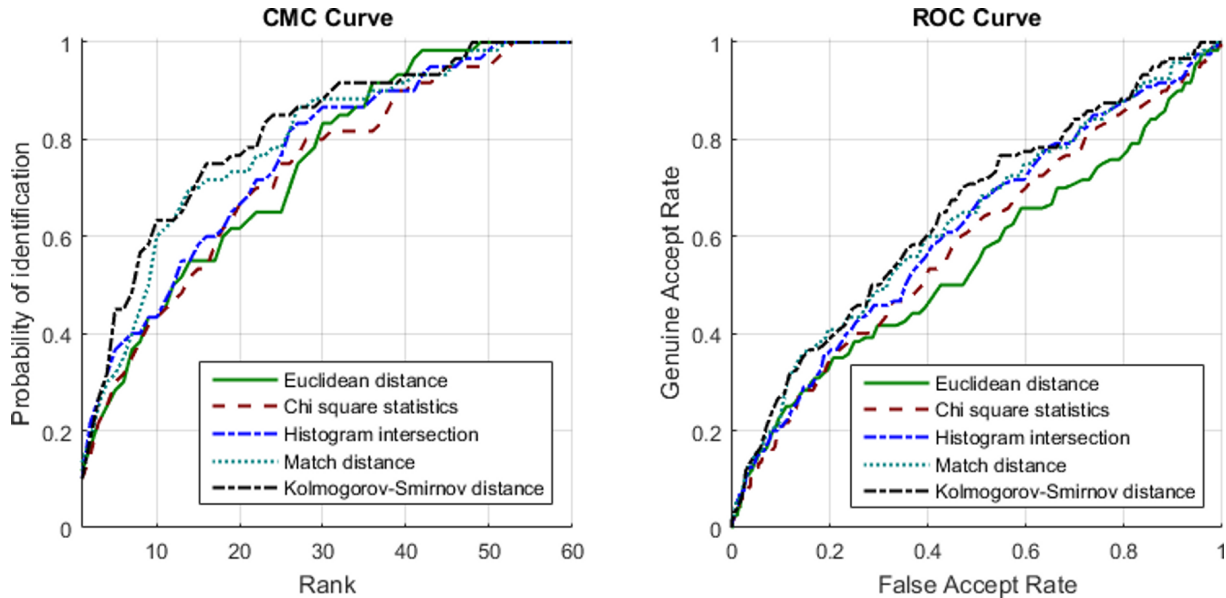[4]http://biplab.unisa.it/MICHE_Contest_ICPR2016/index.php

Fig. 9. CMC and ROC curves obtained from the evaluation of the different techniques for colour comparison.

ages contained in the MICHE-I DB are affected by many different noise factors, in particular we addressed: (i) the different colour appearance due to varying illumination conditions and different capturing device characteristics; (ii) the eyelid occlusion, that hides a large part of the iris features.

In order to solve problem (i), a colour normalization technique is applied, namely the *grey world* normalization. The grey world normalization makes the assumption that changes in the lighting spectrum can be modelled by three constant factors applied to the red, green and blue channels of colour (Buenaposada and Baumela). The result of the colour normalization on some sample MICHE-I DB pictures is illustrated in figure 7. We employed a MATLAB implementation for the colour normalization developed by Juan Manuel Perez Rua[5].

Problem (ii) is addressed by selecting a part of the iris that is more likely to be not occluded by eyelids. The original iris images are first processed by the Haindl and Krupika (2015) algorithm for iris segmentation, made available to all MICHE II participants. The resulting iris image is a mapping of the iris from polar to Cartesian coordinates, i.e. a rectangular image of size 100×600 pixels. In these pictures, the eyelid occlusions are mostly located on the two image sides. For this reason, only the central part of the iris is selected, obtaining a region of interest (ROI) of 100×300 pixels (see figure 8).

3.2. Parallelization

It is worth noticing that, in several phases of the proposed method, the image is split in small blocks or decomposed in a number of layers. The operations applied on each block/layer are independent from each other and thus the computation can

---

Table 1. Colour distance performance evaluation.

Technique	RR	AUC	EER
Euclidean distance	0.12	0.55	0.48
Chi square statistics	0.10	0.59	0.44
Histogram intersection	0.10	0.61	0.41
Match distance	0.13	0.63	0.40
Kolmogorov-Smirnov dist.	0.10	0.65	0.40

be parallelized.

For experimental reproducibility, some implementation details are given: (i) ROI size = 100×300 pixels; (ii) the block size in the colour descriptor is of 50×75 pixels; (iii) the number of layers obtained by the image decomposition is 16, 8 from the a^* channel and 8 from the b^*; (iv) the block size in the texture descriptor is of 25×75 pixels.

4. Performance evaluation

For each descriptor, namely the colour, texture, and cluster descriptors, we tested different techniques and/or parameters in order to improve FIRE's performances. In the following, performances are assessed in terms of Cumulative Match Characteristic curve (hereinafter CMC), Receiver Operating Characteristic curve (hereinafter ROC), Recognition Rate (RR), Area Under ROC Curve (AUC), and Equal Error Rate (EER).

4.1. Colour descriptor performance evaluation

We tested different colour distances, namely the euclidean distance, the chi square statistics, the histogram intersection, the match distance and the Kolmogorov-Smirnov distance. The plot in Fig. 9, illustrates the comparative evaluation of the
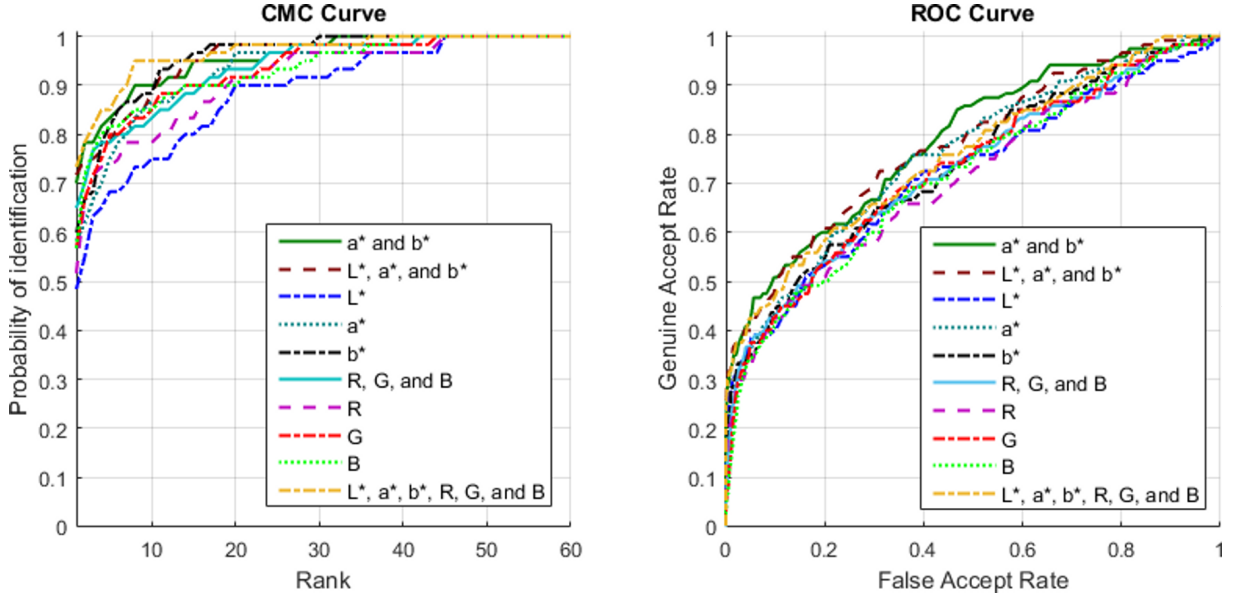
Fig. 10. CMC and ROC curves obtained from the evaluation of the different techniques for texture comparison.

aforementioned techniques. The results in terms of RR, AUC, and EER, are reported in Table 1. The best performing technique, AUC=0.65 and EER=0.40, is the Kolmogorov-Smirnov distance that is thus selected for the final fusion with the texture and cluster descriptors. Although the match distance achieved a better RR (RR=0.13), its behaviour over higher ranks (see the corresponding CMC curve in Fig. 9) is less robust compared to Kolmogorov-Smirnov distance.

It is worth noticing that the reason why the performances are relatively low is that we tested the capability of the colour descriptor of uniquely distinguish a person among others. Of course, since the iris colour is not a very discriminative human characteristic, the RR is low, but combined with the other descriptors, this information will be useful to improve the multi-classifier algorithm performances.

4.2. Texture descriptor performance evaluation

For the texture descriptor, we tested different colour spaces and different numbers of colour channels to be processed by the box-counting technique. In the previous version of the algorithm, we selected the channels a* and b* of the L*a*b* colour space. In Table 2 it is possible to observe the different configurations obtained by combining the L*a*b* and RGB channels. In this case, the experiments confirm that the best combination is $(a*b*)$, performing RR = 0.70, AUC=0.79, and EER=0.32. The corresponding ROC and CMC curves are illustrated in Fig. 10.

4.3. Cluster descriptor performance evaluation

In FIRE's first version, three cluster metrics have been combined to obtain the cluster distance, that is: the centroid horizontal distance, the eccentricity difference, and the orientation difference. Here we test the three aforementioned metrics singularly and also two additional metrics, i.e. the centroid vertical distance and the centroid euclidean distance. In Fig. 11 the plot

Table 2. Texture distance performance evaluation.

Technique	RR	AUC	EER
a* and b*	0.70	0.79	0.32
L*, a*, and b*	0.72	0.78	0.30
L*	0.48	0.72	0.34
a*	0.58	0.75	0.32
b*	0.60	0.74	0.34
R, G, and B	0.65	0.73	0.34
R	0.52	0.71	0.35
G	0.57	0.73	0.33
B	0.57	0.72	0.34
L*, a*, b*, R, G, and B	0.73	0.76	0.33

relative to the metric evaluation, is presented. In Table 3, the results reveal that the centroid euclidean distance performs the best followed by the vertical and horizontal centroid distance. The performances of the eccentricity and orientation difference, instead, are very poor. For this reason, for the fusion step we selected the centroid euclidean distance.

4.4. Achieved improvement and fusion final results

In figure 12 the CMC and ROC curves obtained by the new improved descriptors are illustrated together with the old ones, in order to visualize the achieved improvement.

The fusion of the three classifiers is performed by a weighted sum, where the weights are set to a value proportional to the performance of the corresponding classifier and the sum of the weights is 1. The weights are chosen proportionally to the RR obtained by the single descriptors, i.e. colour = 0.10, texture = 0.70, and cluster = 0.53. The final performances obtained are: RR= 0.70; AUC = 0.80; EER = 0.29.
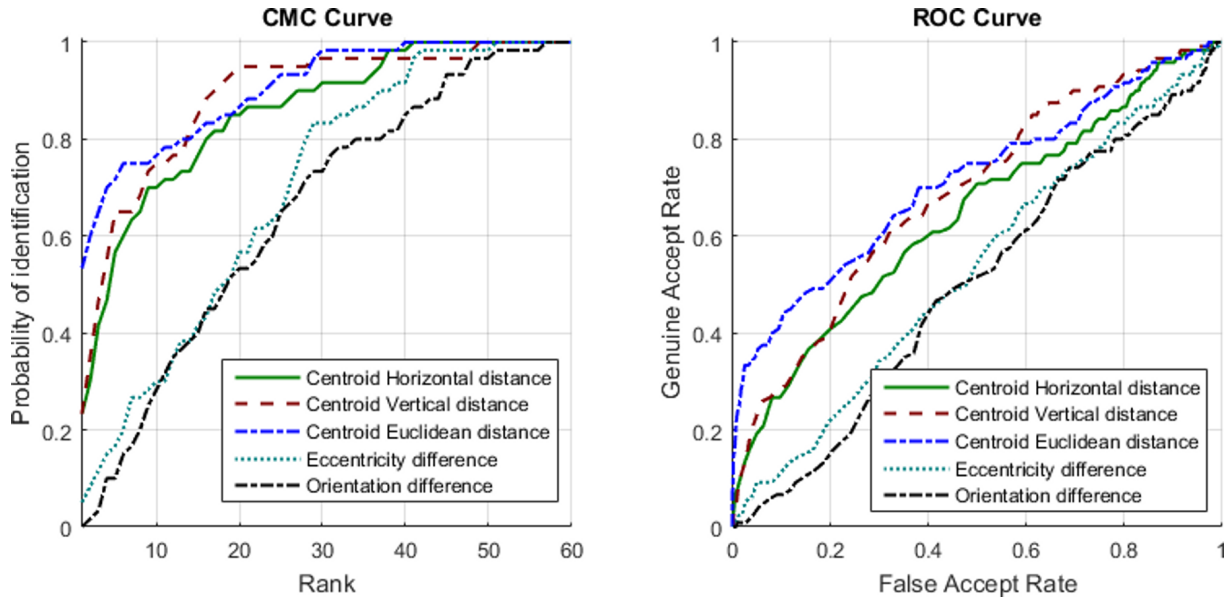
Fig. 11. CMC and ROC curve obtained from the evaluation of the different techniques for cluster comparison.
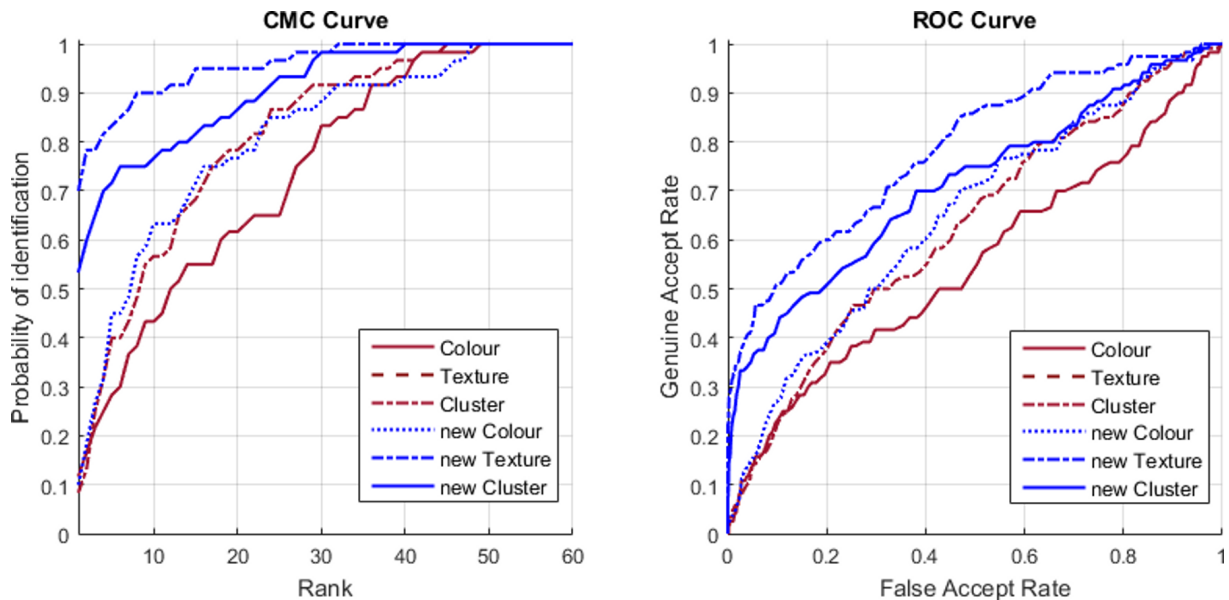

Fig. 12. CMC and ROC curves obtained from the comparative evaluation of the old descriptors versus the new ones. Please notice that the old and the new Texture descriptor coincide.

Table 3. Cluster distance performance evaluation.

Technique	RR	AUC	EER
Centroid horizontal dist.	0.23	0.64	0.40
Centroid vertical dist.	0.23	0.69	0.36
Centroid Euclidean dist.	0.53	0.71	0.35
Eccentricity difference	0.05	0.53	0.49
Orientation difference	0	0.50	0.49

4.5. Computational time

The performance evaluation discussed in the previous section, has been obtained by comparing 60 Probe images against 60 Gallery images, for a total of 3600 comparisons. We performed the test on a machine with following characteristics:

- DELL R610
    - Processor: 2 x Intel(R) Xeon(R) CPU L5640 @ 2.27GHz (6 cores);
    - RAM: 32GB;

The total computational time is of about 355", for an average computational time for a single comparison of about 0.0986".

The limited computational time of the presented approach has two main advantages, the suitability for comparisons one-to-many on large databases and, more importantly, the applicability in the context of real-time user authentication on mobile

devices. Due to the still limited computational power of mobile devices, is of paramount importance developing solution for fast biometric recognition.

5. Conclusion

FIRE is a novel approach for fast noisy iris recognition. It has been tested on a very challenging database, namely the MICHE-I DB composed by iris images collected by different mobile devices. FIRE was first presented on the occasion of the MICHE II challenge evaluation held in 2016. In this paper we investigated new techniques in order to improve the algorithm. Three descriptors have been developed. The colour descriptor employs the Kolmogorov-Smirnov distance to compare two histograms and achieved an AUC of 0.65. The texture descriptor is based on the computation of the box-counting dimension on several layers in which the iris image is decomposed. The best performances were obtained using the a* and b* channels of the CIE 1976 L*a*b* colour space, with AUC = 0.79. Finally, the cluster descriptor achieved an AUC of 0.71 by computing the euclidean distance between the cluster centroids.

Fusion is performed at score level and the resulting multi-classifier algorithm achieved an AUC of 0.80. Although far to be perfect, this result is very interesting considering that FIRE only exploits the iris area for feature extraction while some of the other approaches presented in MICHE II, that achieved better performances, also integrate information from the periocular area. Last but not the least, the computational time of FIRE is very limited thanks to the high parallelization of the code, that is of paramount importance when dealing with automatic and real-time user authentication.

References

Abate, A.F., Frucci, M., Galdi, C., Riccio, D., 2015. Bird: Watershed based {IRis} detection for mobile devices. Pattern Recognition Letters 57, 43 – 51. URL: http://www.sciencedirect.com/science/article/pii/S0167865514003341, doi:http://dx.doi.org/10.1016/j.patrec.2014.10.017. mobile Iris {CHallenge} Evaluation part I (MICHE I).

Barra, S., Casanova, A., Narducci, F., Ricciardi, S., 2015. Ubiquitous iris recognition by means of mobile devices. Pattern Recognition Letters 57, 66 – 73. URL: http://www.sciencedirect.com/science/article/pii/S0167865514003286, doi:http://dx.doi.org/10.1016/j.patrec.2014.10.011. mobile Iris {CHallenge} Evaluation part I (MICHE I).

Buenaposada, J.M., Baumela, L., . Variations of grey world for face tracking.

Conti, M., Zachia-Zlatea, I., Crispo, B., 2011. Mind how you answer me!: Transparently authenticating the user of a smartphone when answering or placing a call, in: Proceedings of the 6th ACM Symposium on Information, Computer and Communications Security, ACM, New York, NY, USA. pp. 249–259. URL: http://doi.acm.org/10.1145/1966913.1966945, doi:10.1145/1966913.1966945.

Daugman, J., 2004. How iris recognition works. IEEE Transactions on Circuits and Systems for Video Technology 14, 21–30. doi:10.1109/TCSVT.2003.818350.

DeMarsico, M., Galdi, C., Nappi, M., Riccio, D., 2014. Firme: Face and iris recognition for mobile engagement. Image and Vision Computing 32, 1161 – 1172. URL: http://www.sciencedirect.com/science/article/pii/S0262885614000055, doi:http://dx.doi.org/10.1016/j.imavis.2013.12.014.

DeMarsico, M., Nappi, M., Riccio, D., 2012. Noisy iris recognition integrated scheme. Pattern Recognition Letters 33, 1006 – 1011. URL: http://www.sciencedirect.com/science/article/pii/S0167865511002832, doi:http://dx.doi.org/10.1016/j.patrec.2011.09.010. noisy Iris

Challenge Evaluation {II} - Recognition of Visible Wavelength Iris Images Captured At-a-distance and On-the-move.

DeMarsico, M., Nappi, M., Riccio, D., Wechsler, H., 2015. Mobile iris challenge evaluation (miche)-i, biometric iris dataset and protocols. Pattern Recognition Letters 57, 17 – 23. URL: http://www.sciencedirect.com/science/article/pii/S0167865515000574, doi:http://dx.doi.org/10.1016/j.patrec.2015.02.009. mobile Iris {CHallenge} Evaluation part I (MICHE I).

Fahmi, P.N.A., Kodirov, E., Choi, D.J., Lee, G.S., Azli, A.M.F., Sayeed, S., 2012. Implicit authentication based on ear shape biometrics using smartphone camera during a call, in: 2012 IEEE International Conference on Systems, Man, and Cybernetics (SMC), pp. 2272–2276. doi:10.1109/ICSMC.2012.6378079.

Haindl, M., Krupika, M., 2015. Unsupervised detection of non-iris occlusions. Pattern Recognition Letters 57, 60 – 65. URL: http://www.sciencedirect.com/science/article/pii/S0167865515000604, doi:http://dx.doi.org/10.1016/j.patrec.2015.02.012. mobile Iris {CHallenge} Evaluation part I (MICHE I).

Mohanta, T.K., Mohapatra, S., 2014. Article: Development of multimodal biometric framework for smartphone authentication system. International Journal of Computer Applications 102, 6–11. Full text available.

Nickel, C., Wirtl, T., Busch, C., 2012. Authentication of smartphone users based on the way they walk using k-nn algorithm, in: Intelligent Information Hiding and Multimedia Signal Processing (IIH-MSP), 2012 Eighth International Conference on, pp. 16–20. doi:10.1109/IIH-MSP.2012.11.

Poh, N., Hadid, A., Marcel, S., McCool, C., Matejka, P., Levy, C., Tresadern, P., Cootes, T.F., 2013. Mobile biometrics: Combined face and voice verification for a mobile platform. IEEE Pervasive Computing 12, 79–87. doi:doi.ieeecomputersociety.org/10.1109/MPRV.2012.54.

Proenca, H., Alexandre, L.A., 2007. The nice.i: Noisy iris challenge evaluation - part i, in: Biometrics: Theory, Applications, and Systems, 2007. BTAS 2007. First IEEE International Conference on, pp. 1–4. doi:10.1109/BTAS.2007.4401910.

Raghavendra, R., Raja, K.B., Pflug, A., Yang, B., Busch, C., 2013. 3d face reconstruction and multimodal person identification from video captured using smartphone camera, in: Technologies for Homeland Security (HST), 2013 IEEE International Conference on, pp. 552–557. doi:10.1109/THS.2013.6699063.

Rubner, Y., Tomasi, C., Guibas, L.J., 2000. The earth mover's distance as a metric for image retrieval. International Journal of Computer Vision 40, 99–121. URL: http://dx.doi.org/10.1023/A:1026543900054, doi:10.1023/A:1026543900054.

Saevanee, H., Bhattarakosol, P., 2009. Authenticating user using keystroke dynamics and finger pressure, in: 2009 6th IEEE Consumer Communications and Networking Conference, pp. 1–2. doi:10.1109/CCNC.2009.4784783.

Shen, H.C., Wong, A.K., 1983. Generalized texture representation and metric. Computer Vision, Graphics, and Image Processing 23, 187 – 206. URL: http://www.sciencedirect.com/science/article/pii/0734189X83901123, doi:http://dx.doi.org/10.1016/0734-189X(83)90112-3.

Swain, M.J., Ballard, D.H., 1991. Color indexing. International Journal of Computer Vision 7, 11–32. URL: http://dx.doi.org/10.1007/BF00130487, doi:10.1007/BF00130487.

Tapia, J.E., Perez, C.A., Bowyer, K.W., 2016. Gender classification from the same iris code used for recognition. IEEE Transactions on Information Forensics and Security 11, 1760–1770. doi:10.1109/TIFS.2016.2550418.